HHS Public Access

Author manuscript

J Mol Neurosci. Author manuscript; available in PMC 2017 May 01.

Published in final edited form as:

J Mol Neurosci. 2016 May ; 59(1): 1–17. doi:10.1007/s12031-015-0711-6.

Neuronal Hemoglobin Expression and Its Relevance to Multiple Sclerosis Neuropathology

Nolan Brown[#1], **Kholoud Alkhayer**[#1], **Robert Clements**[1], **Naveen Singhal**[1], **Roger Gregory**[2], **Sausan Azzam**[3], **Shuo Li**[1,2], **Ernest Freeman**[1], and **Jennifer McDonough**[1]

[1] Department of Biological Sciences and School of Biomedical Sciences, Kent State University, Kent, OH 44242, USA

[2] Department of Chemistry and Biochemistry, Kent State University, Kent, OH, USA

[3] Proteomics Core, Case Western Reserve University, Cleveland, OH, USA

[#] These authors contributed equally to this work.

Abstract

Multiple sclerosis (MS) is characterized by demyelination and progressive neurological disability. Previous studies have reported defects to mitochondria in MS including decreased expression of nuclear encoded electron transport chain subunit genes and inhibition of respiratory complexes. We previously reported increased levels of the hemoglobin β subunit (Hbb) in mitochondrial fractions isolated from postmortem MS cortex compared to controls. In the present study, we performed immunohistochemistry to determine the distribution of Hbb in postmortem MS cortex and identified proteins which interact with Hbb by liquid chromatography tandem mass spectrometry (LC-MS/MS). We found that Hbb was enriched in pyramidal neurons in internal layers of the cortex and interacts with subunits of ATP synthase, histones, and a histone lysine demethylase. We also found that Hbb is present in the nucleus and that expression of Hbb in SH-SY5Y neuroblastoma cells increased trimethylation of histone H3 on lysine 4 (H3K4me3), a histone mark that regulates cellular metabolism. These data suggest that Hbb may be a part of a mechanism linking neuronal energetics with epigenetic changes to histones in the nucleus and may provide neuroprotection in MS by supporting neuronal metabolism.

Keywords

Multiple sclerosis; Hemoglobin expression; Pyramidal neurons; Mass spectrometry; Mitochondrial genes; Histone methylation

Introduction

Multiple sclerosis (MS) is a neurodegenerative disease characterized by the demyelination and deterioration of neurons within the central nervous system (CNS) (Noseworthy et al. 2000). In MS, axonal and neuronal degeneration and inflammatory demyelination accumulate over time, resulting in progressive neurological disability (Bjartmar et al. 2000;

Jennifer McDonough jmcdonou@kent.edu.

De Stefano et al. 2001). Historically, MS was considered a white matter disease and the majority of research concerning MS was focused on understanding autoimmune demyelination. However, it has been established that cortical pathology, including extensive gray matter lesions and cortical atrophy, contribute to the progression of MS (Bo et al. 2006; Inglese et al. 2004; Fisher et al. 2008). The mechanisms involved in cortical pathology are not clear, but current hypotheses describe dysfunction of the mitochondria in the cortex in MS. In studies analyzing postmortem brain tissue, the expression of genes involved in mitochondrial respiration has been found to be altered in normal appearing gray matter (NAGM) in MS brains compared to NAGM in non-diseased brains (Dutta et al. 2006; Pandit et al. 2009; Witte et al. 2013). In a subsequent proteomic analysis of mitochondria in MS and control cortical tissue, hemoglobin β (Hbb) was found to be expressed in neurons and was more abundant in MS postmortem cortex compared to non-diseased cortex (Broadwater et al. 2011).

Until recently, erythrocytes were believed to be the only cell type to contain hemoglobin. The function of hemoglobin in red blood cells is to transport and exchange oxygen (O_2) and carbon dioxide (CO_2) in tissues. In red blood cells, hemoglobin exists as a heterotetramer of two hemoglobin α (Hba) and two hemoglobin β (Hbb) subunits. However, studies have now shown that various cell types other than erythrocytes, such as macrophages, epithelial cells, and neurons, also contain hemoglobin (Rahaman and Straub 2013). The discovery of Hba and/or Hbb expression in diverse cell types suggests that they have other roles in addition to their role in O_2 and CO_2 transport. Hemoglobins contain a heme-prosthetic group (Fe-protoporphyrin IX) which binds not only O_2 and CO_2 but also nitric oxide (NO), allowing them to also participate in redox and dioxygenase reactions (Reeder et al. 2010). In mesangial cells of the kidney, hemoglobin has been shown to act as an anti-oxidant (Nishi et al. 2008). Separate functions have also been described for the α and β subunits in some cell types. In macrophages, the hemoglobin β minor subunit is expressed without the α subunit and acts to scavenge NO (Liu et al. 1999). In vascular endothelial cells, Hba is expressed and has been shown to regulate NO release necessary for vasodilation when O_2 concentrations are low (Straub et al. 2012). It is clear that hemoglobin has evolved to carry out diverse physiological functions in many different cell types. The role of hemoglobin in neurons in the CNS is still not clear. In order to better understand the function of Hbb and its potential role in providing neuroprotection in MS, we have analyzed the cortical distribution of Hbb by immunohistochemistry. We have also performed co-immunoprecipitation (Co-IP) experiments with an Hbb antibody followed by liquid chromatography tandem mass spectrometry (LC-MS/MS) to identify proteins interacting with Hbb in the MS cortex and in cultured primary neurons.

Methods

Immunofluorescent Staining

Postmortem MS and control cortical brain tissue was obtained under IRB protocol from the Rocky Mountain MS Center and the Human Brain and Spinal Fluid Resource Center at UCLA. For immunofluorescent staining, frozen tissue blocks were fixed in 4 % paraformaldehyde for 24 h and cut 30 μm thick using a vibratome. Cortical tissue from five

MS and four control brains was analyzed. Donor and tissue characteristics including age, sex, postmortem interval (PMI), and brain region are shown in Table 1. Blocking buffer was prepared as 1× phosphate-buffered saline (PBS) with 0.5 % Triton X-100 and 3 % normal donkey serum. Samples were blocked in blocking buffer for 1 h and then primary antibodies were diluted in blocking buffer and applied to samples overnight at 4 °C. Primary antibodies were applied in the following concentrations: Hbb (Aviva Systems Biology, San Diego, CA) 1:250, neurofilament (SMI32) (Calbiochem, Billerica, MA) 1:500, and tyrosine hydroxylase (Santa Cruz Biotechnologies, Dallas, TX) 1:250. Secondary antibodies were also applied in blocking buffer at 4 °C for 2 h. All secondary antibodies were obtained from Invitrogen (Carlsbad, CA) and were applied at a concentration of 1:500. Secondary antibodies used are as follows: donkey anti-rabbit Alexafluor 488, donkey anti-goat Alexafluor 488, donkey anti-mouse Alexafluor 555, and donkey anti-goat Alexafluor 555. After incubation of secondary antibodies, samples were soaked in 10 mM cupric sulfate, 10 mM ammonium acetate buffer for 90 min to quench autofluorescence. Samples were mounted on microscope slides using Vectashield mounting medium for fluorescence with DAPI (Vector Laboratories, Burlingame, CA). Mounted samples were viewed with a Fluoview 1000 confocal microscope and imaged using the bundled software.

Immunostaining with neurofilament (SMI32) allowed the visualization of the cortical layers in each tissue block analyzed. Only sections containing all layers of the cortex with neural projections streaming perpendicular to the pial surface were included. With SMI32 as a guide to ensure that all layers of the cortical section were analyzed, contiguous ×20 objective fields were imaged from the outer edge of the cortex to the white matter. Image stacks spanning the depth of the tissue sections were acquired and the fields were stitched together with Fluoview software to create a map of the cortex spanning from the pial surface to cortical layer VI. SMI32 and Hbb immunoreactive neurons were counted in the external and internal cortical layers for sections from five MS and four control brains with Image J (Rasband 1997).

Primary Neuronal Cultures

All animal procedures were approved by the Institutional Animal Care and Use Committee (IACUC) of Kent State University. Primary neuronal cultures were isolated from E17 Sprague Dawley rat brains. Briefly, cerebral cortices were dissected from the whole fetal rat brain and meninges carefully removed. The rat cerebral cortex was mechanically dissociated in EMEM containing 10 % FBS using fire polished Pasteur pipettes and then passed through 70 μm pore-sized mesh. Cells were then pelleted by centrifugation of 100×*g* for 10 min at 4 °C and resuspended with neurobasal medium supplemented with B27 and N2. Cells were plated on poly-D-lysine-coated tissue culture dishes and maintained at 37 °C and 5 % CO_2 in a humidified incubator. Primary neurons were cultured for 10 days before protein isolation. Media was changed after 3 days to eliminate any hemoglobin from blood contamination. Total protein was isolated for identification of hemoglobin interacting proteins by co-IP followed by LC-MS/MS. To confirm the presence of hemoglobin in our cultures, some cells were incubated on coverslips and immunostained with antibodies to hemoglobin (Pierce Biotechnology, Rockford, IL) and neurofilament (Chemicon, Temecula, CA) followed by the appropriate fluorescent secondary antibodies Alexafluor 488 or

Alexafluor 555 (both from Invitrogen, Carlsbad, CA). Western blotting of protein isolated from our cultured rat primary neurons also confirmed the presence of a hemoglobin 16-kDa band (not shown). Immunostained cells were imaged with a Fluoroview 1000 confocal microscope.

Protein Extraction and Co-IP for Mass Spectrometry

For co-IP experiments, total protein was isolated from cortical gray matter tissue from an MS brain and from rat primary neuronal cultures. Tissue or cells were homogenized with a mini-homogenizer for 60 s in five volumes of extraction buffer. Extraction buffer consisted of 20 mM HEPES, pH 7.5, 100 mM NaCl, 0.05 % Triton X-100, 1 mM dithiothreitol (DTT), 5 mM sodium β-glycerophosphate, 0.5 mM sodium orthovanadate, 1 mM EDTA, 0.5 mM phenylmethylsulfonyl fluoride (PMSF), 10 μg/mL aprotinin, 5 μg/mL leupeptin, and 2 μg/mL pepstatin. The samples were then spun at 12,000×*g* for 15 min at 4 °C. The supernatant was taken and spun again at 12,000×*g* for 10 min at 4 °C. The supernatant was kept as the protein sample. Co-IP was performed with the protein isolated using the Pierce™ Classic Magnetic IP/Co-IP Kit (Thermo Scientific, Waltham, MA). In order to form the Hbb and antibody immune complex, 1.0 mg of protein extract was incubated with 10 μg of an Hbb antibody (Aviva Systems Biology, San Diego, CA). Protein isolated from rat primary neurons was incubated with 10 μg of a hemoglobin antibody (Pierce Biotechnology, Rockford, IL). Protein was also immunoprecipitated with non-specific IgG as a control. The protein and antibodies were incubated for 2 h at room temperature, with the total reaction diluted to 500 μL in IP Lysis/Wash Buffer. IP Lysis/Wash Buffer consisted of 0.025 M Tris, 0.15 M NaCl, 0.001 M EDTA, 1 % NP40, and 5 % glycerol at pH 7.4. After complex formation, 25 μL of washed magnetic beads were added to the complex solution and incubated at room temperature for 1 h. The beads were washed with 500 μL IP Lysis/Wash Buffer and then with 500 μL of ultrapure water. The sample was eluted with 100 μL of low-pH elution buffer for 10 min at room temperature and then neutralized.

Eluted proteins from the Co-IP were resuspended in SDS-PAGE sample buffer and denatured at 95 °C for 5 min. The sample was run on a NuPAGE 4-12 % Bis Tris Gel (Invitrogen, Carlsbad, CA) and Coomassie stained to visualize protein bands. The gel was washed and destained in distilled water. The protein lane was cut out of the gel and destained with 500 μL of 1:1 ACN (acetonitrile) and 100 mM ABC (ammonium bicarbonate) solution for 2–6 h. Next, the gel piece was dehydrated and hydrated with 200 μL 100 % ACN and 200 μL 100 mM ABC, respectively. Disulfide bonds were then reduced with 10 mM DTT at 56 °C for 45 min, and free cysteines were alkylated with 55 mM IAA (iodoacetamide) in the dark at RT for 45 min. The gel piece was then swelled in 50 mM ABC containing freshly prepared 10 ng/μL trypsin (Promega, Madison, WI, sequencing-grade) and digested overnight at 37 °C. Subsequently, peptides were extracted 50 % ACN/25 mM ABC/5 % FA (formic acid) and dried in SpeedVac.

Reverse Phase LC-MS/MS Analysis and Protein Identification

For gel-based tandem mass spectrometry analysis, digested peptides were reconstituted with 0.1 % formic acid and analyzed by LC-MS/MS using an LTQ-Orbitrap Elites mass spectrometer (Thermo Scientific, Waltham, MA) equipped with a nanoAcquity™ Ultra-high

pressure liquid chromatography system (Waters). The mobile phases included aqueous phase A (0.1 % FA in water) and organic phase B (0.1 % FA in 85 % ACN). Tryptic peptides were loaded onto a nanoACQUITY UPLC desalting trap column (180 μm × 20 mm nano column, 5 μm, 100 A°, Waters). Subsequently, peptides were resolved in a nanoACQUITY UPLC reversed phase column (75 μm × 250 mm nano column, 1.7 μm, 100 A°; Waters). Liquid chromatography was carried out using a gradient elution of 1–90 % of organic phase over 90 min at ambient temperature. Peptides were then introduced into the mass spectrometer via a nano-electrospray ion source at a flow rate of 0.3 μL/min. Full scan MS spectra were acquired at a resolution of 60,000 followed by 20 collision-induced dissociation (CID) fragmentations in a data-dependent manner. The dynamic exclusion list was confined to a maximum of 500 entries, with exclusion duration of 45 s and mass accuracy of 10 ppm for the precursor monoisotopic mass.

For protein identification, the LC-MS/MS raw files were acquired using the Thermo X-calibur software (Thermo Scientific, Waltham, MA) and searched by Mascot (version 2.3.01, Matrix Science) against the human Uniprot (71,434 sequences) database. Search settings were as follows: trypsin enzyme specificity; mass accuracy window for precursor ion, 10 ppm; mass accuracy window for fragment ions, 0.8 Da; variable modifications including carbamidomethylation of cysteines, one missed cleavage, and oxidation of methionine. The search results were then filtered using the cutoff criteria of p value ≤0.05.

Hbb Expression Construct and Transfections

Total RNA were extracted from approximately 50 mg human brain tissue using a SV total RNA isolation system (Promega, Madison, WI) according to manufacturer's instructions. The quantity and quality of RNA were checked with a ND1000 Nanodrop spectrophotometer (Nanodrop Technologies, Wilmington, DE). Reverse transcription to produce cDNA was performed with a Brilliant III ultrafast SYBR Green QRT-PCR kit (Agilent Technologies, Santa Clara, CA). Full-length human Hbb cDNA was amplified by PCR from human brain cDNA using the following primer pairs: Hbb F 5′ATCCTCGAGTGCTTCTGACACAACTGTGTTCACT 3′ and Hbb R 5′ ATCCCGGGTGGACAGCAAGAAAGCGAGCTT 3′. The resulting PCR product was cloned into pEGFP (Clontech Laboratories) and then subcloned into the XhoI and NheI sites of the pVitro2 mammalian expression vector (Invivogen, San Diego, CA). The constructed plasmid was confirmed by sequencing and the insert showed 100 % sequence similarity with the Hbb sequence from NCBI [hemoglobin β (NM_000518.4)].

Human SH-SY5Y neuroblastoma cells were cultured in 1:1 mixture of EMEM and F-12 medium (Sigma-Aldrich, St. Louis, MO) with 10 % FBS (MidSci, St. Louis, MO) in a 37 °C incubator with 5 % CO_2. pVitro2 and pVitro2-Hbb constructs were purified and transfected into SH-SY5Y cells with TransIt Express transfection reagent (Mirus, Madison, WI) according to manufacturer's instructions. The pVitro2 and pVitro2-Hbb plasmids were incubated with the TransIt transfection reagent for 30 min to allow DNA complexes to form. The complexes were then added to SH-SY5Y cells already seeded on 100 mm culture plates to 80 % confluency and incubated for 48 h. After 48 h, protein was isolated and Western blotting was performed to measure levels of Hbb expression and histone methylation.

Western Blotting

Proteins were separated by SDS polyacrylamide gel electrophoresis on NuPage 4–12 % Bis-Tris gels (Invitrogen, Carlsbad, CA) and transferred to nitrocellulose. Blots were then incubated in primary antibody overnight and then in the appropriate HRP-conjugated secondary antibody for 2 h and immunoreactivity was detected with Luminol (Santa Cruz Biotechnologies, Dallas, TX). For quantitation of nuclear and mitochondrial Hbb protein levels in MS and control postmortem tissue, protein was isolated and fractionated according to the method of Pallotti and Lenaz (2007). Six MS and six control cortical gray matter tissue samples were analyzed (Table 1). The purity of fractions was determined by Western blotting with antibodies to the mitochondrial membrane protein aralar (BD Biosciences, Franklin Lakes, NJ) and the neuronal nuclear marker NeuN (Chemicon International, Temecula, CA). Western blots were also performed with an antibody to the astrocyte marker GFAP (not shown). Any samples exhibiting increased GFAP indicative of astrogliosis or a change in cellularity indicated by decreased NeuN were eliminated. Western blotting was performed with an antibody to Hbb (Aviva Systems Biology, San Diego, CA) and relative Hbb levels were determined after normalization to either NeuN for nuclear fractions or aralar for mitochondrial fractions. To confirm identification of Hbb interacting proteins, Western blots were performed with protein immunoprecipitated with antibodies to Hbb or non-specific IgG. Blots were incubated with antibodies to Hbb (Aviva Systems Biology, San Diego, CA), ATP5A1 (Novex Life Technologies, Waltham, MA), and histone H3 (Abcam, Cambridge, MA). To measure Hbb and H3K4me3 levels in transfected SH-SY5Y cells, blots were incubated with antibodies to either Hbb (Aviva Systems Biology, San Diego, CA) or histone H3 trimethylated on lysine 4 (H3K4me3) (Abcam, Cambridge, MA). Hbb levels were normalized to GAPDH (Millipore, Temecula, CA) and H3K4me3 was normalized to histone H3. Protein levels were determined by densitometry with Image J from at least two independent experiments. Statistical significance of changes in protein levels was determined with a Student's t test with $p \leq 0.05$ considered significant.

Results

To understand the distribution of hemoglobin in the cortex and to determine whether this distribution is altered in MS, we performed immunofluorescent staining with antibodies to hemoglobin and the neuronal marker neurofilament (SMI32) in cortical sections obtained from five MS and four control brains (Table 1). A representative confocal image showing the subdivisions of the cortex ascertained by SMI32 immunostaining in motor cortex from an MS sample is shown in Fig. 1a. Representative confocal images showing colocalization of Hbb and SMI32 in neurons in MS cortical sections are shown in Fig. 1b. We did not find any statistically significant difference between MS and control brains in the overall percentage of Hbb + cells or in the cortical distribution of Hbb. We identified a total of 703 SMI32+ neurons from immunostained sections from the motor and parietal cortex across five MS brains and found that 33 % were also immunoreactive for Hbb. For control brains, 534 SMI32 positive neurons were identified across four brains and 172 also expressed Hbb (32 %). In addition, we found that Hbb expression was enriched in the internal layers of the cortex (layers IV–VI) compared to external layers (layers I–III) in both MS and control brains. For MS brains, 300 SMI32 positive neurons were identified in the external layers of

the cortex, and 67 were also immunoreactive for Hbb (22 %). In the internal layers, 403 SMI32 positive neurons were identified and 167 expressed Hbb (42 %). For controls, in external layers, 49 of 197 SMI32 positive neurons expressed Hbb (25 %). In the internal layers, 337 SMI32 positive neurons were counted and 123 also expressed Hbb (36 %). Most Hbb containing neurons exhibited pyramidal cell morphology. Hbb expression was found to be localized predominantly in the cytoplasm of these cells, but nuclear staining was also detected as shown in Fig. 1c. Weak staining for Hbb was observed in the nucleus, but not in the nucleolus in pyramidal neurons in both MS and control cortical tissue. It has been reported that SMI32, which stains non-phosphorylated neurofilament-H, is a marker of dystrophic neurons and axons, and is indicative of axonal damage. In our hands we did not observe a difference in neurofilament staining with SMI32 or with the SMI31 antibody which stains phosphorylated neurofilament in postmortem tissue. We also stained tissue blocks with SMI31 and Hbb and obtained similar results (data not shown).

In addition to SMI32 and Hbb labeling, sections of MS and control brains were stained for tyrosine hydroxylase (TH) and Hbb (Fig. 1d). TH catalyzes the rate limiting step of the formation of catecholamines, which include the neurotransmitters dopamine, adrenaline, and noradrenaline. TH has also been localized within interneurons, and thus can be used as a histochemical marker for interneurons (Benavides-Piccione and DeFelipe 2007). These TH positive interneurons do not synthesize catecholamines, but appear to be GABAergic. An abundance of TH labeled neurons was found in the MS samples, each with morphologies consistent with interneurons. TH labeled neurons did not appear to contain Hbb; however, some TH labeled neurons were observed to form what appeared to be synapses to cells which did contain Hbb (Fig. 1d). TH labeled neurons appeared to contact the cell bodies of Hbb expressing neurons as opposed to dendrites, suggesting these TH expressing neurons are GABAergic inhibitory interneurons, as inhibitory synapses often target cell bodies instead of dendrites. Benavides-Piccione and DeFelipe (2007) state that the most common cell type targeted by interneurons are pyramidal cells.

We did not observe any significant changes in the numbers of neurons expressing Hbb in MS cortex compared to controls. To determine whether levels of Hbb protein were changed between MS and control brains, we performed Western blotting with mitochondrial and nuclear protein isolated from six MS and six control cortical gray matter samples as shown in Fig. 2. The relative purity of protein fractions was determined by Western blotting with antibodies to the mitochondrial membrane protein aralar and the neuronal nuclear marker NeuN. A representative Western blot demonstrating purity of fractionation is shown in Fig. 2a for a subset of samples. Consistent with our previous study, we found that mean Hbb levels were increased by 29 % in mitochondrial fractions isolated from MS cortical samples compared to controls (Broadwater et al. 2011) (Fig. 2b, d). We also measured levels of Hbb in nuclear fractions and found that Hbb levels were reduced on average by 38 % in MS nuclear fractions compared to controls (Fig. 2c, d).

We then performed co-IP experiments with an antibody to Hbb and total cell extracts from motor cortex from an MS brain to identify proteins which interact with Hbb. Fifteen proteins including Hbb itself were identified by LC-MS/MS ($p \leq 0.05$). Table 2 describes the proteins identified which coimmunoprecipitated with Hbb. All peptide sequences assigned are listed,

with their respective observed and expected peptide masses and ion scores. The accession number for each protein is listed with their respective exponentially modified protein abundance index (emPAI), queries matched, and mass. The emPAI is a semi-quantitative estimate of the relative abundance of proteins in the sample. It is the number of peptides per protein normalized by the theoretical number of peptides. Proteins low in abundance will have low emPAI scores. Five of the Hbb interacting proteins identified in the postmortem sample were mitochondrial, including ATP synthase subunits alpha and beta (ATP5A1 and ATP5B), mitochondrial malate dehydrogenase (MDH2), ADP/ATP translocase 4 (SLC25A31), and a mitochondrial phosphate carrier (SLC25A3), suggesting that Hbb is associated with mitochondria. We also identified several histone proteins including histone H3 (HIST2H3A) and lysine-specific demethylase 8 (KDM8), which is a histone demethylase, suggesting that Hbb may be involved in regulating histone methylation. Western blotting confirmed that Hbb eluted after immunoprecipitation with the Hbb antibody as expected (Fig. 3) but Hbb did not elute after immunoprecipitation with a non-specific IgG antibody. Other Hbb interacting proteins identified by co-IP followed by LC-MS/MS including ATP5A1 and histone H3 were also confirmed by Western blot as shown in Fig. 3.

Because the protein isolated from the human postmortem cortical sample would contain protein not only from neurons but also from other cell types that express hemoglobin including red blood cells, vascular endothelial cells, and macrophages, we repeated the co-IP combined with LC-MS/MS with total protein isolated from cultured rat primary neurons. It has been reported previously that primary neurons express hemoglobin (Schelshorn et al. 2009). To confirm that our cultured neurons expressed hemoglobin, we first performed immunofluorescent staining with hemoglobin and neurofilament antibodies. Confocal images in Fig. 4 show that hemoglobin (Hb) and neurofilament (NF) are co-expressed in these cells. Neuron-specific hemoglobin interacting proteins identified by LC-MS/MS are shown in Table 3 and are consistent with those identified in the human postmortem cortical gray matter sample. Hemoglobin interacting proteins in rat primary neurons overlapped with many of the mitochondrial and nuclear proteins identified in the postmortem sample including Atp5a1, Atp5b, Mdh2, Slc25a3, and histones (Table 3). We also identified 2-oxoglutarate dehydrogenase in primary neurons which is of interest since many histone demethylases require 2-oxoglutarate as a cofactor (Gut and Verdin 2013; Salminen et al. 2014). These data provide further evidence that hemoglobin may be involved in mediating signals between mitochondria and the nucleus in neurons.

To test whether Hbb could be regulating histone methylation, we transfected human SH-SY5Y neuroblastoma cells, which do not express endogenous Hbb, with either the empty expression vector (pVitro2) or expression vector driving Hbb expression (pVitro2-Hbb) and measured histone H3 methylation. After 48 h, cytoplasmic and nuclear extracts were isolated. Western blotting was performed with cytoplasmic protein and an antibody to Hbb to show that Hbb was being expressed from the pVitro2-Hbb expression construct in the neuroblastoma cells after transfection (Fig. 5a). We then performed Western blotting with nuclear extracts and an antibody to H3K4me3 and found that levels of this methylated histone were increased by almost twofold in pVitro2-Hbb transfected cells after normalization to histone H3 levels (Fig. 5b, c).

Discussion

The presence of hemoglobin mRNA and protein within neuronal cells of the rodent and human CNS has been confirmed in several studies (Richter et al. 2009; Biagoli et al. 2009; Schelshorn et al. 2009; Broadwater et al. 2011), but the function of hemoglobin in cortical neurons is still not clear. Hemoglobin may serve a direct role in delivering oxygen to mitochondria in neurons. The association of hemoglobin with mitochondria is consistent with such a role (Shephard et al. 2014). However, hemoglobin may also have other functions in neurons. In order to better understand the role of hemoglobin in the CNS and its relevance to MS pathology, we first examined the cortical distribution of Hbb and its expression relative to the neuronal marker SMI32 in postmortem MS cortical tissue. The cerebral cortex can be subdivided anatomically into six layers based on the types of neurons within each layer and organization of their projections. Layer I contains almost no neurons. Cortical layers II and III contain neurons which form intracortical connections, projecting to other cortical neurons either in the same hemisphere or to the opposite hemisphere through the corpus callosum. Layer IV receives input from the thalamus, and neurons in layers V and VI project for the most part to subcortical regions including the spinal cord (DeFelipe and Farinas 1992). We found that the majority of neurons that contained Hbb and SMI32 appeared to be pyramidal neurons. Pyramidal neurons are glutamatergic and can be identified by their large size, apical dendrites, long axons, and pyramidal shape. They are generally found in cortical layers III and V but are also occasionally located in others layers. Hbb immunoreactivity in these cells was strongest in the cell body but weak staining also appeared in the nucleus and was absent in the nucleolus. These data are consistent with the study by Richter et al. 2009 which found hemoglobin immunoreactivity in cortical pyramidal neurons in rodent and human brains and the Biagoli et al. (2009) study which also reported hemoglobin expression in the cytoplasm and nucleus, but not in the nucleolus, in dopaminergic neurons.

Nonpyramidal cells are generally short axon cells which reside in middle layers of the cortex and are often inhibitory, signaling through GABAergic neurotransmission. Many of these interneurons synthesize TH. In contrast to a study by Biagoli et al. (2009), who found hemoglobin expression in TH containing neurons in the substantia nigra, we did not find any colocalization of TH and Hbb, but we did find that TH labeled neurons appeared to synapse to the soma of Hbb containing cells. This observation was consistent with the fact that TH labeled interneurons have been shown to preferentially synapse with pyramidal cells (Benevides-Piccione and DeFelipe 2007). The discrepancy between our study and the Biagoli et al. (2009) study is most likely due to the brain regions analyzed. We analyzed TH and Hbb colocalization in interneurons in the cortex while the Biagoli study analyzed deeper structures including mesencephalic dopaminergic neurons.

The significance of the increased distribution of Hbb expressing pyramidal neurons in internal cortical layers is not clear, but it may be a result of the large size and axonal projections of these cells. Neurons with longer projections require increased ATP to maintain ion homeostasis and conduction of nerve impulses over long distances. Our data show that Hbb overexpression in SH-SY5Y neuroblastoma cells increased H3K4me3, a histone mark that is present in actively transcribed regions of chromatin and regulates

expression of oxidative phosphorylation genes (Singhal et al. 2015). A role for hemoglobin in mitochondrial respiration is supported by a study by Biagoli et al. (2009) which suggested that alterations in hemoglobin expression affect cellular energetics, since dopaminergic cell lines over expressing α- and β-globin subunits exhibited changes in oxygen homeostasis and alterations in the expression of mitochondrial genes. One explanation for the enrichment of Hbb expression in projection neurons in deeper cortical layers could be to maintain an adequate supply of ATP by upregulating H3K4me3 and expression of genes necessary for oxidative phosphorylation.

Our data suggest that changes in Hbb subcellular localization may contribute to MS pathology by exacerbating the effects of demyelination on neuronal energetics. Pyramidal cells in deeper cortical layers (layers V and VI) project to subcortical regions including the thalamus and spinal cord. As a result of the longer distances these axons traverse, they are more likely to be exposed to inflammatory insults and demyelination. Axons that are demyelinated redistribute sodium channels in order to maintain conductivity (England et al. 1991; Waxman 2006). As a result, these neurons require additional ATP in order to maintain ion homeostasis and neurotransmission. In addition to metabolic stress induced by demyelination, neurons are further compromised in MS by a dysregulation of mitochondrial genes and impaired energetics. Mitochondrial abnormalities including decreased expression of nuclear encoded electron transport chain subunit genes, the neuronal mitochondrial metabolite N-acetylaspartate, and the mitochondrial biogenesis factor PPARGC1a have been reported in cortical neurons in MS in studies analyzing postmortem tissue even in areas with no overt pathology (Witte et al. 2013; Li et al. 2013). Indications of metabolic changes and a dysfunction of mitochondrial respiration in MS cortical gray matter have also been observed in vivo in magnetic resonance spectroscopy studies (Ge et al. 2004; Cader et al. 2007). Our data suggest that there is a change in Hbb subcellular localization in MS, with increased Hbb in mitochondria and decreased Hbb in the nucleus. A dysregulation of Hbb transport into the nucleus in pyramidal neurons in MS may lead to a reduction in H3K4me3 and decreased expression of genes involved in mitochondrial respiration. This mechanism may contribute to the previously reported reductions in H3K4me3 and decreased expression of mitochondrial respiratory complexes in MS cortical neurons (Singhal et al. 2015; Dutta et al. 2006). Depletion of nuclear Hbb in MS may lead to an inability for neurons to meet the increased demands for energy as a result of demyelination.

It is not clear how Hbb is regulating methylation of H3K4me3 but it is known that histone H3 demethylases are dioxygenases that can be regulated by mitochondrial metabolites (Salminen et al. 2014; Gut and Verdin 2013). These dioxygenases catalyze the oxidation of carbon-hydrogen bonds and require O_2 (Vissers et al. 2014). Since one of the main functions of hemoglobin is to bind O_2, it may regulate histone H3 methylation by sequestering oxygen from histone demethylases, preventing the dioxygenase reaction and histone demethylation. We found that overexpressing Hbb alone increased H3K4me3 suggesting that although in erythrocytes the α- and β subunits function as a heterotetramer, these genes may have evolved separate functions and may act independent from one another in some cells. This idea is consistent with data showing that only Hba is expressed in vascular endothelial cells where it participates in a dioxygenase reaction which regulates NO release independent of Hbb (Straub et al. 2012). Hbb can also form a tetramer (HbH) which has a higher binding

affinity for O_2 than the $\alpha_2\beta_2$ heterotetramer (Bellelli et al. 2006). Similarly, Hbb may act independently from Hba in cortical pyramidal cells and may provide a mechanism to regulate histone demethylation, chromatin conformation, and gene expression in response to changes in cellular metabolism and O_2 consumption.

We have found that Hbb is expressed in cortical pyramidal neurons and is enriched in internal cortical layers in MS. We have also found that Hbb interacts with subunits of ATP synthase, an ADP/ATP translocase, histones, and a histone lysine demethylase. Overexpression of Hbb in SH-SY5Y cells increased levels of trimethylated histone H3. Taken together these data suggest that Hbb may be a part of a mechanism linking mitochondrial energetics with epigenetic changes to histones and gene expression changes in the nucleus.

Acknowledgments

We would like to thank the Rocky Mountain MS Center which is funded by the National Multiple Sclerosis Society and the Brain and Spinal Cord Resource Center at UCLA for tissue. This research was partially funded by NIH Grant R21NS075645 (JM and EF) and from funds from the College of Arts and Sciences at Kent State University (JM).

References

Bellelli A, Brunori M, Miele AE, Panetta G, Vallone B. The allosteric properties of hemoglobin: insights from natural and site directed mutants. Curr Protein Pept Sci. 2006; 7:17–45. [PubMed: 16472167]

Benavides-Piccione R, DeFelipe J. Distribution of neurons expressing tyrosine hydroxylase in the human cerebral cortex. J Anat. 2007; 211(2):212–22. [PubMed: 17593221]

Biagioli M, Pinto M, Cesselli D, Zaninello M, Lazarevic D, Roncaglia P, Simone R, Vlachouli C, Plessy C, Bertin N, Beltrami A, Kobayashi K, Gallo V, Santoro C, Ferrer I, Rivella S, Beltrami CA, Carninci P, Raviola E, Gustincich S. Unexpected expression of α- and β-globin in mesencephalic dopaminergic neurons and glial cells. Proc Natl Acad Sci U S A. 2009; 106:15454–15459. [PubMed: 19717439]

Bjartmar C, Kidd G, Mörk S, Rudick R, Trapp BD. Neurological disability correlates with spinal cord axonal loss and reduced N-acetyl-aspartate in chronic multiple sclerosis patients. Ann Neurol. 2000; 48:893–901. [PubMed: 11117546]

Bö L, Geurts JJ, Mörk SJ, van der Valk P. Grey matter pathology in multiple sclerosis. Acta Neurol Scand Suppl. 2006; 183:48–50. [PubMed: 16637929]

Broadwater L, Pandit A, Azzam S, Clements R, Vadnal J, Yong VW, Freeman EJ, Gregory RB, McDonough J. Analysis of the mitochondrial proteome in multiple sclerosis cortex. Biochim Biophys Acta. 2011; 1812:630–641. [PubMed: 21295140]

Cader S, Johansen-Berg H, Wylezinska M, Palace J, Behrens TE, Smith S, Matthews PM. Discordant white matter N-acetylasparate and diffusion MRI measures suggest that chronic metabolic dysfunction contributes to axonal pathology in multiple sclerosis. Neuroimage. 2007; 36(1):19–27. [PubMed: 17398118]

DeFelipe J, Farinas I. The pyramidal neuron of the cerebral cortex: morphological and chemical characteristics of the synaptic inputs. Prog Neurobiol. 1992; 39(6):563–607. [PubMed: 1410442]

De Stefano N, Narayanan S, Francis GS, Arnaoutelis R, Tartaglia MC, Antel JP, Matthews PM, Arnold DL. Evidence of axonal damage in the early stages of multiple sclerosis and its relevance to disability. Arch Neurol. 2001; 58(1):65–70. [PubMed: 11176938]

Dutta R, McDonough J, Yin X, Peterson J, Chang A, Torres T, Gudz T, Macklin WB, Lewis DA, Fox RJ, Rudick R, Mirnics K, Trapp BD. Mitochondrial dysfunction as a cause of axonal degeneration in multiple sclerosis patients. Ann Neurol. 2006; 59:478–489. [PubMed: 16392116]

England JD, Gamboni F, Levinson SR. Increased numbers of sodium channels form along demyelinated axons. Brain Res. 1991; 548(1-2):334–7. [PubMed: 1651145]

Fisher E, Lee JC, Nakamura K, Rudick RA. Gray matter atrophy in multiple sclerosis: a longitudinal study. Ann Neurol. 2008; 64(3):255–65. [PubMed: 18661561]

Ge Y, Gonen O, Inglese M, Babb JS, Markowitz CE, Grossman RI. Neuronal cell injury precedes brain atrophy in multiple sclerosis. Neurology. 2004; 62(4):624–7. [PubMed: 14981182]

Gut P, Verdin E. The nexus of chromatin regulation and intermediary metabolism. Nature. 2013; 502(7472):489–98. doi:10.1038/nature12752, Review. [PubMed: 24153302]

Inglese M, Ge Y, Filippi M, Falini A, Grossman RI, Gonen O. Indirect evidence for early widespread gray matter involvement in relapsing-remitting multiple sclerosis. Neuroimage. 2004; 21:1825–1829. [PubMed: 15050603]

Li S, Clements R, Sulak M, Gregory R, Freeman E, McDonough J. Decreased NAA in gray matter is correlated with decreased availability of acetate in white matter in postmortem multiple sclerosis cortex. Neurochem Res. 2013; 38(11):2385–96. [PubMed: 24078261]

Liu L, Zeng M, Stamler JS. Hemoglobin induction in mouse macrophages. Proc Natl Acad Sci U S A. 1999; 96(12):6643–7. [PubMed: 10359765]

Nishi H, Inagi R, Kato H, Tanemoto M, Kojima I, Son D, Fujita T, Nangaku M. Hemoglobin is expressed by mesangial cells and reduces oxidant stress. J Am Soc Nephrol. 2008; 19(8):1500–8. [PubMed: 18448584]

Noseworthy JH, Lucchinetti C, Rodriguez M, Weinshenker BG. Multiple sclerosis. N Engl J Med. 2000; 343(13):938–52. [PubMed: 11006371]

Pallotti F, Lenaz G. Isolation and subfractionation of mitochondria from animal cells and tissue culture lines. Methods Cell Biol. 2007; 80:3–44. [PubMed: 17445687]

Pandit A, Vadnal J, Houston S, Freeman E, McDonough J. Impaired regulation of electron transport chain subunit genes by nuclear respiratory factor 2 in multiple sclerosis. J Neurol Sci. 2009; 279:14–20. [PubMed: 19187944]

Rahaman MM, Straub AC. The emerging roles of somatic globins in cardiovascular redox biology and beyond. Redox Biol. 2013; 1:405–10. [PubMed: 24191233]

Rasband, WS. ImageJ, U. S. National institutes of health. Bethesda, Maryland, USA: 1997-2014. http://imagej.nih.gov/ij/

Reeder BJ. The redox activity of hemoglobins: from physiologic functions to pathologic mechanisms. Antioxid Redox Signal. 2010; 13(7):1087–123. doi:10.1089/ars.2009.2974. [PubMed: 20170402]

Richter F, Meurers BH, Zhu C, Medvedeva VP, Chesselet M-F. Neurons express hemoglobin α- and β-chains in rat and human brains. J Comp Neurol. 2009; 515:538–547. [PubMed: 19479992]

Salminen A, Kauppinen A, Hiltunen M, Kaarniranta K. Krebs cycle intermediates regulate DNA and histone methylation: epigenetic impact on the aging process. Ageing Res Rev. 2014; 16:45–65. [PubMed: 24910305]

Schelshorn DW, Schneider K, Weber AW, Kruger D, Dittgen C, Burgers HF, Sabouri F, Gassler N, Bach A, Martin H, Maurer MH. Expression of hemoglobin in rodent neurons. J Cerebr Blood Flow Metab. 2009; 29:585–595.

Shephard F, Greville-Heygate O, Marsh O, Anderson S, Chakrabarti L. A mitochondrial location for haemoglobins—dynamic distribution in ageing and Parkinson's disease. Mitochondrion. 2014; 14(1):64–72. doi:10.1016/j.mito.2013.12.001. [PubMed: 24333691]

Singhal NK, Li S, Arning E, Alkhayer K, Clements R, Sarcyk Z, Dassanayake RS, Brasch NE, Freeman EJ, Bottiglieri T, McDonough J. Changes in methionine metabolism and his-tone H3 Trimethylation are linked to mitochondrial defects in multiple sclerosis. J Neurosci. 2015; 35(45): 15170–15186. [PubMed: 26558787]

Straub AC, Lohman AW, Billaud M, Johnstone SR, Dwyer ST, Lee MY, Bortz PS, Best AK, Columbus L, Gaston B, Isakson BE. Endothelial cell expression of haemoglobin α regulates nitric oxide signalling. Nature. 2012; 491(7424):473–7. [PubMed: 23123858]

Vissers MC, Kuiper C, Dachs GU. Regulation of the 2-oxoglutarate-dependent dioxygenases and implications for cancer. Biochem Soc Trans. 2014; 42(4):945–51. [PubMed: 25109984]

Waxman SG. Ions, energy and axonal injury: towards a molecular neurology of multiple sclerosis. Trends Mol Med. 2006; 12(5):192–5. [PubMed: 16574486]

Witte ME, Nijland PG, Drexhage JA, Gerritsen W, Geerts D, van Het Hof B, Reijerkerk A, de Vries HE, van der Valk P, van Horssen J. Reduced expression of PGC-1α partly underlies mitochondrial changes and correlates with neuronal loss in multiple sclerosis cortex. Acta Neuropathol. 2013; 125(2):231–43. [PubMed: 23073717]

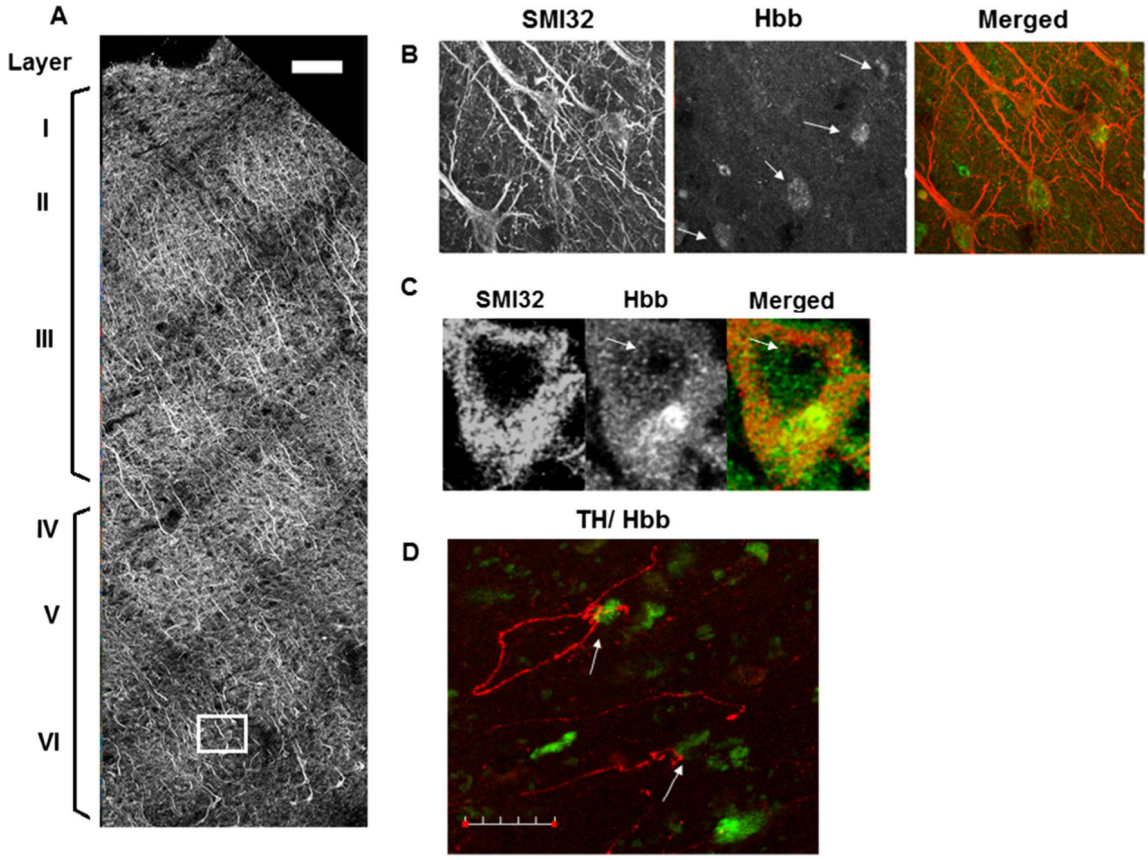

Fig. 1.

Cortical distribution of Hbb expressing pyramidal neurons in MS cortex. **a** Representative confocal image from MS motor cortex immunostained with antibodies to neurofilament (SMI32) and Hbb. Sequential ×20 confocal images were acquired from the pial surface extending through cortical layer VI and stitched into a single image. Cortical layers were visualized by SMI32 staining shown in grayscale. *Scale bar* represents 100 μm. **b** Panel shows the boxed region in A at higher magnification. SMI32 and Hbb immunoreactivity can be seen in pyramidal neurons denoted by *arrows.* SMI32 and Hbb channels are shown in grayscale and the merged image on the right shows colocalization of SMI32 (*red fluorescence*) and Hbb (*green fluorescence*). SMI32 and Hbb positive cells were counted in cortical tissue sections from five MS brains. We found that on average 33 % of SMI32+ cells were also immunoreactive for Hbb. In external layers of the cortex (layers I–III), 22 % of SMI32+ neurons were Hbb+. In cortical layers IV–VI, the internal cortical layers, 42 % of SMI32 neurons also expressed Hbb. **c** Hbb expression is observed in the nucleus but not in the nucleolus (denoted by *arrows*) in pyramidal cells. **d** Representative confocal image showing an MS cortical section immunostained with antibodies to TH (*red fluorescence*) and Hbb (*green fluorescence*). *Arrows* denote TH positive axons appearing to contact cell bodies of Hbb positive cells. *Scale bar* represents 30 μm

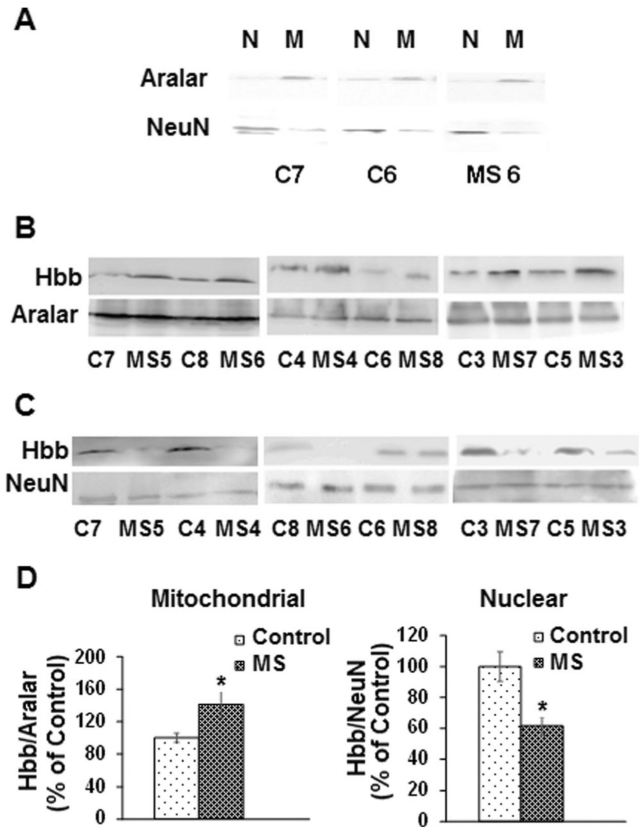

Fig. 2.

The subcellular localization of Hbb is altered in MS samples. **a** Representative Western blot demonstrating the purity of mitochondrial and nuclear fractions isolated from control and MS postmortem cortical gray matter. Nuclear (*N*) and mitochondrial (*M*) fractions isolated from control and MS samples were blotted with antibodies to the neuronal nuclear marker NeuN and the mitochondrial marker aralar. **b** Representative Western blots for Hbb and aralar in mitochondrial fractions isolated from MS cortical samples compared to controls. **c** Representative Western blots for Hbb and NeuN show decreased Hbb in MS nuclear fractions compared to controls. **d** Quantitation shows that average Hbb levels are increased in mitochondrial fractions and decreased in nuclear fractions isolated from MS cortical gray matter compared to controls. *Error bars* represent SEM. $*p < 0.05$

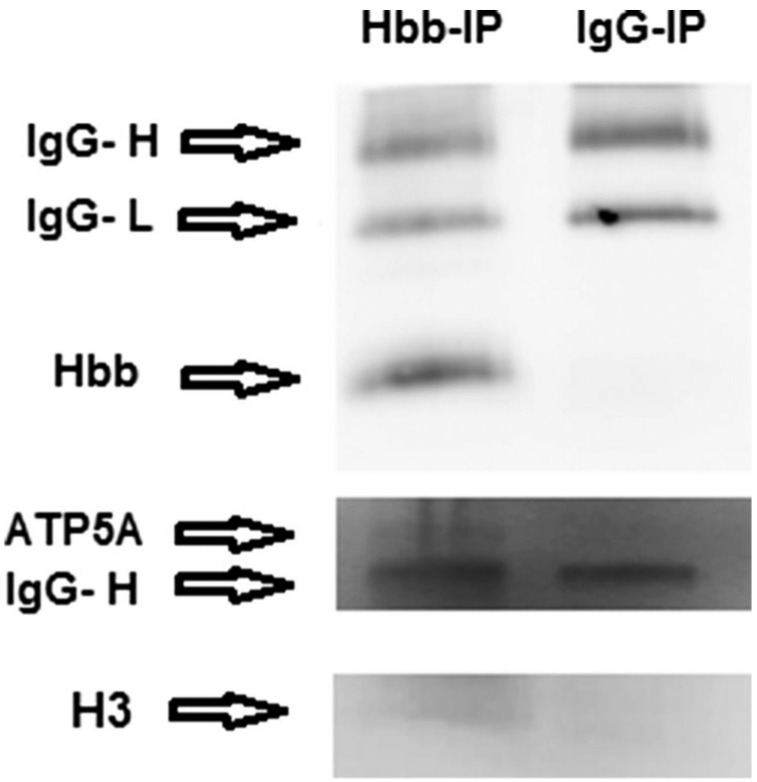

Fig. 3.

Confirmation of proteins interacting with Hbb that were identified by mass spectrometry. Western blotting shows that Hbb, ATP5A1, and histone H3 were pulled down in the IP experiment with the Hbb antibody but not with the non-specific IgG antibody. *Arrows* denote bands for Hbb (16 kDa), ATP5A1 (55 kDa), and histone H3 (13 kDa) on separate blots. Because this protein was immunoprecipitated with an Hbb antibody, IgG heavy and light chains (IgG-H and IgG-L) are present at 50 and ~25 kDa

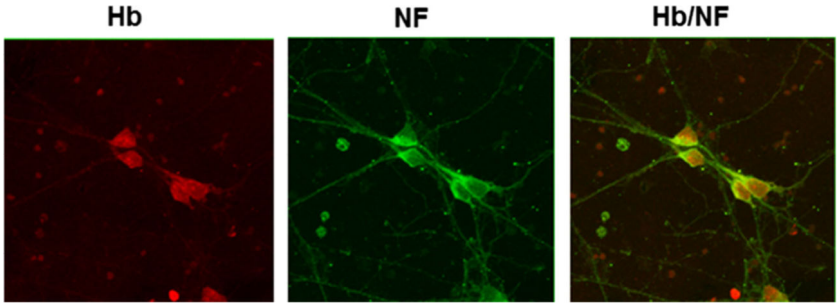

Fig. 4.

Hemoglobin is expressed in cultured rat primary neurons. Cultured neuronal cells were immunostained with antibodies to hemoglobin (*Hb*) and neurofilament (*NF*). The merged image shows Hb (*red fluorescence*) and NF (*green fluorescence*) colocalization

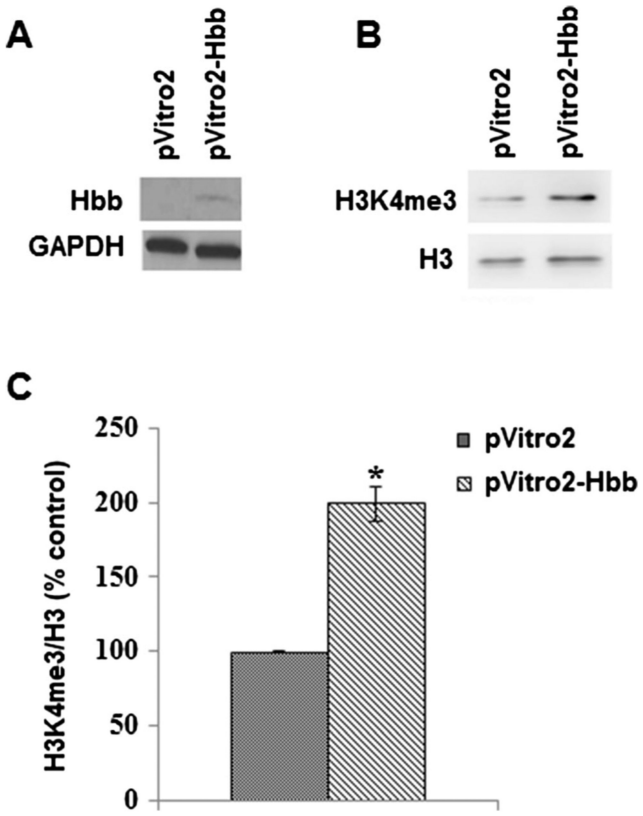

Fig. 5.

Hbb expression regulates histone H3 trimethylation. **a** Western blotting shows that the Hbb subunit is expressed in SH-SY5Y cells transfected with pVitro2-Hbb. **b** Representative Western blot demonstrates that levels of H3K4me3 are increased in nuclear extracts isolated from SH-SY5Y cells transfected with pVitro2-Hbb compared to control cells transfected with vector alone. **c** Quantitation for H3K4me3 levels in SH-SY5Y cells transfected with either empty vector pVitro2 or pVitro2-Hbb was performed by densitometry from two separate experiments. *Error bars* represent SEM, $*p < 0.05$

Table 1

Donor and tissue characteristics

Sample	Age (years)	Sex	PMI (h)	Region of cortex
MS 1	79	F	7.0	Parietal
MS 2	69	M	12.0	Motor
*MS 3	63	F	23.0	Frontal
*MS 4	78	F	7.8	Parietal
*MS 5	79	F	7.4	Parietal
*MS 6	53	F	3.0	Parietal
*MS 7	61	F	6.0	Parietal
*MS 8	36	F	3.0	Parietal
C1	83	F	17.6	Motor
C2	74	M	13.4	Frontal
*C3	74	F	18.0	Frontal
*C4	67	M	22.0	Motor
*C5	74	F	4.5	Frontal
*C6	80	M	9.5	Parietal
*C7	59	F	19.5	Frontal
*C8	35	F	9.3	Parietal

Table 2

Proteins interacting with Hbb identified by co-IP followed by mass spectrometry

Protein							
1	**P62805**	Mass, 11360	Score, 626	Matches, 30(30)	Sequences, 6(6)	emPAI, 7.38	
	Histone H4 Homo sapiens GN=HIST1H4A						
	Query	Observed	Mr(expt)	Mr(calc)	Score	Expect	Peptide
	6197	714.3464	713.3391	713.3385	39	0.00043	R.TLYGFGG.-
	9328	495.2934	988.5722	988.5706	49	0.00011	K.VFLENVIR.D
	10541	567.7756	1133.5366	1133.5353	44	0.00036	R.DAVTYTEHAK.R
	10865	590.8145	1179.6144	1179.6135	61	8.7e–006	R.ISGLIYEETR.G
	11693	663.3817	1324.7488	1324.7463	47	0.00015	R.DNIQGITKPAIR.R
	11698	663.8536	1325.6926	1325.6901	50	9.1e–005	K.TVTAMDVVYALK.R
2	**Q6FI13**	Mass, 14087	Score, 535	Matches, 19(19)	Sequences, 6(6)	emPAI, 3.55	
	Histone H2A type 2-A Homo sapiens GN=HIST2H2AA3						
	Query	Observed	Mr(expt)	Mr(calc)	Score	Expect	Peptide
	7540	419.2148	836.4150	836.4140	27	0.018	R.KGNYAER.V
	7851	425.7671	849.5196	849.5184	34	0.00064	R.HLQLAIR.N
	8013	431.2011	860.3876	860.3875	22	0.037	R.NDEELNK.L
	8951	472.7695	943.5244	943.5240	66	4.5e–006	R.AGLQFPVGR.V
	13753	644.3956	1930.1650	1930.1615	68	1.9e–007	K.VTIAQGGVLPNIQAVLLPK.K
	15856	983.8522	2948.5348	2948.5317	64	3.3e–006	R.VGAGAPVYMAAVLEYLTAEILELAGNAAR.D
3	**P16104**	Mass, 15135	Score, 379	Matches, 16(16)	Sequences, 6(6)	emPAI, 3.14	
	Histone H2A.x Homo sapiens GN=H2AFX						
	Query	Observed	Mr(expt)	Mr(calc)	Score	Expect	Peptide
	7851	425.7671	849.5196	849.5184	34	0.00064	R.HLQLAIR.N
	8013	431.2011	860.3876	860.3875	22	0.037	R.NDEELNK.L
	8463	449.2010	896.3874	896.3876	22	0.019	K.ATQASQEY.-
	8951	472.7695	943.5244	943.5240	66	4.5e–006	R.AGLQFPVGR.V
	14651	1136.1930	2270.3714	2270.3726	53	5.6e–006	K.LLGGVTIAQGGVLPNIQAVLLPK.K
	15814	972.5350	2914.5832	2914.5804	75	1.3e–007	R.VGAGAPVYLAAVLEYLTAEILELAGNAAR.D
4	**P68871**	Mass, 15988	Score, 508	Matches, 17(17)	Sequences, 7(7)	emPAI, 2.84	
	Hemoglobin subunit beta Homo sapiens GN=HBB						
	Query	Observed	Mr(expt)	Mr(calc)	Score	Expect	Peptide
	8849	466.7641	931.5136	931.5127	29	0.016	K.SAVTALWGK.V
	9039	476.7588	951.5030	951.5025	24	0.032	M.VHLTPEEK.S
	10637	575.3421	1148.6696	1148.6666	40	0.00042	K.VVAGVANALAHK.Y
	11403	637.8672	1273.7198	1273.7183	34	0.0028	R.LLVVYPWTQR.F
	11629	657.8362	1313.6578	1313.6575	72	6e–007	K.VNVDEVGGEALGR.L
	12030	689.8539	1377.6932	1377.6929	36	0.0034	K.EFTPPVQAAYQK.V
	14036	1037.9760	2073.9374	2073.9354	92	5.2e–009	R.FFESFGDLSTPDAVMGNPK.V
5	**Q5QNW6**	Mass, 13912	Score, 496	Matches, 29(29)	Sequences, 7(7)	emPAI, 6.23	
	Histone H2B type 2-F Homo sapiens GN=HIST2H2BF						

Protein							
	Query	Observed	Mr(expt)	Mr(calc)	Score	Expect	Peptide
	4201	585.2880	584.2807	584.2806	18	0.033	K.YTSSK.-
	7272	408.7325	815.4504	815.4501	34	0.0055	R.EIQTAVR.L
	7404	414.7150	827.4154	827.4137	38	0.00088	K.HAVSEGTK.A
	9047	477.3063	952.5980	952.5957	20	0.026	R.LLLPGELAK.H
	10795	390.2040	1167.5902	1167.5884	48	0.00016	K.QVHPDTGISSK.A
	11347	633.3250	1264.6354	1264.6339	36	0.0029	R.KESYSVYVYK.V
	13282	888.4092	1774.8038	1774.8018	(79)	1.1e–007	K.AMGIMNSFVNDIFER.I
6	**Q71DI3**	Mass, 15379	Score, 273	Matches, 16(16)	Sequences, 3(3)	emPAI, 1.22	
	Histone H3.2 Homo sapiens GN=HIST2H3A						
	Query	Observed	Mr(expt)	Mr(calc)	Score	Expect	Peptide
	6224	715.4102	714.4029	714.4024	32	0.0088	K.DIQLAR.R
	7467	416.2508	830.4870	830.4861	64	4.9e–006	K.STELLIR.K
	7833	850.4313	849.4240	849.4232	50	0.00012	R.EIAQDFK.T
7	**P25705**	Mass, 59714	Score, 185	Matches, 6(6)	Sequences, 3(3)	emPAI, 0.17	
	ATP synthase subunit alpha, mitochondrial Homo sapiens GN=ATP5A1						
	Query	Observed	Mr(expt)	Mr(calc)	Score	Expect	Peptide
	9641	513.8013	1025.5880	1025.5869	28	0.0095	K.AVDSLVPIGR.G
	12779	788.3994	1574.7842	1574.7788	77	2.6e–007	R.ILGADTSVDLEETGR.V
	12923	812.9507	1623.8868	1623.8832	50	8.8e–005	R.TGAIVDVPVGEELLGR.V
8	**P40926**	Mass, 35481	Score, 169	Matches, 2(2)	Sequences, 1(1)	emPAI, 0.09	
	Malate dehydrogenase, mitochondrial Homo sapiens GN=MDH2						
	Query	Observed	Mr(expt)	Mr(calc)	Score	Expect	Peptide
	13347	897.0498	1792.0850	1792.0822	97	2e–010	K.VAVLGASGGIGQPLSLLLK.N
9	P06576	Mass, 56525	Score, 101	Matches, 2(2)	Sequences, 1(1)	emPAI, 0.06	
	ATP synthase subunit beta, mitochondrial Homo sapiens GN=ATP5B						
	Query	Observed	Mr(expt)	Mr(calc)	Score	Expect	Peptide
	13877	994.5219	1987.0292	1987.0262	68	2.2e–006	R.AIAELGIYPAVDPLDSTSR.I
10	**Q9H0C2**	Mass, 34999	Score, 99	Matches, 3(3)	Sequences, 2(2)	emPAI, 0.20	
	ADP/ATP translocase 4 Homo sapiens GN=SLC25A31						
	Query	Observed	Mr(expt)	Mr(calc)	Score	Expect	Peptide
	7931	428.7490	855.4834	855.4814	24	0.017	K.TAVAPIER.V
	12294	723.8759	1445.7372	1445.7343	60	1.6e–005	R.YFPTQALNFAFK.D
11	**P10412**	Mass, 21852	Score, 90	Matches, 7(7)	Sequences, 3(3)	emPAI, 0.53	
	Histone H1.4 Homo sapiens GN=HIST1H1E						
	Query	Observed	Mr(expt)	Mr(calc)	Score	Expect	Peptide
	7180	406.2014	810.3882	810.3872	25	0.02	K.GTGASGSFK.L
	9215	487.3066	972.5986	972.5968	31	0.0036	R.SGVSLAALKK.A
	10346	554.2881	1106.5616	1106.5608	45	0.0005	K.ALAAAGYDVEK.N
12	**Q00325**	Mass, 40069	Score, 47	Matches, 2(2)	Sequences, 1(1)	emPAI, 0.08	
	Phosphate carrier protein, mitochondrial Homo sapiens GN=SLC25A3						
	Query	Observed	Mr(expt)	Mr(calc)	Score	Expect	Peptide

Protein							
	11909	681.3629	1360.7112	1360.7099	44	0.00063	R.IQTQPGYANTLR.D
13	**P69905**	Mass, 15248	Score, 41	Matches, 2(2)	Sequences, 1(1)	emPAI, 0.22	
	Hemoglobin subunit alpha OS=Homo sapiens GN=HBA1						
	Query	Observed	Mr(expt)	Mr(calc)	Score	Expect	Peptide
	12621	510.5836	1528.7290	1528.7270	33	0.0048	K.VGAHAGEYGAEALER.M
14	**Q8N371**	Mass, 47240	Score, 24	Matches, 2(2)	Sequences, 1(1)	emPAI, 0.07	
	Lysine-specific demethylase 8 Homo sapiens GN=KDM8						
	Query	Observed	Mr(expt)	Mr(calc)	Score	Expect	Peptide
	7597	421.7583	841.5020	841.5021	22	0.038	K.LEKTVPR.L
15	**P0C0S8**	Mass, 14083	Score, 92	Matches, 3(3)	Sequences, 2(2)	emPAI, 0.54	
	Histone H2A type 1 Homo sapiens GN=HIST1H2AG						
	Query	Observed	Mr(expt)	Mr(calc)	Score	Expect	Peptide
	9506	472.7698	943.5250	943.5240	39	0.0024	R.AGLQFPVGR.V
	15653	972.5334	2914.5784	2914.5804	61	3.9e–006	R.VGAGAPVYLAAVLEYLTAEILELAGNAAR.D
16	**Q5QNW6**	mass, 13912	score, 34	matches, 3(3)	sequences, 2(2)	emPAI, 0.55	
	Histone H2B type 2-F Homo sapiens GN=HIST2H2BF						
	Query	Observed	Mr(expt)	Mr(calc)	Score	Expect	Peptide
	8107	408.7327	815.4508	815.4501	33	0.0074	R.EIQTAVR.L
	9609	477.3055	952.5964	952.5957	18	0.025	R.LLLPGELAK.H

Table 3

Proteins interacting with hemoglobin in cultured primary neurons

Protein							
1	**P02091**	Mass, 15969	Score, 4251	Matches, 126(126)	Sequences, 14(14)	emPAI, 121.67	
	Hemoglobin subunit beta-1 Rattus norvegicus GN=Hbb						
	Query	Observed	Mr(expt)	Mr(calc)	Score	Expect	Peptide
	5761	739.4104	738.4031	738.4024	28.51	0.0025	HLDNLK
	8065	912.4783	911.471	911.4712	43.63	0.0001	VHLTDAEK
	8111	458.2562	914.4978	914.4974	45.01	0.00012	AAVNGLWGK
	9911	1090.589	1089.5817	1089.5818	53.78	2.30E–05	VINAFNDGLK
	10208	561.8355	1121.6564	1121.6557	71.86	6.80E–08	VVAGVASALAHK
	10248	563.786	1125.5574	1125.5567	28.79	0.005	LHVDPENFR
	10938	609.8459	1217.6772	1217.6768	72.89	2.20E–07	KVINAFNDGLK
	11335	637.8666	1273.7186	1273.7183	51.57	1.90E–05	LLVVYPWTQR
	11482	649.8201	1297.6256	1297.6263	75.84	8.30E–08	VNPDDVGGEALGR
	12152	699.33	1396.6454	1396.6445	58.4	4.10E–06	EFTPCAQAAFQK
	12274	711.897	1421.7794	1421.7779	63.1	1.60E–06	VVAGVASALAHKYH
	12695	505.5738	1513.6996	1513.6984	27.73	0.0054	GTFAHLSELHCDK
	13339	572.0121	1713.0145	1713.0124	39.19	0.00012	LLGNMIVIVLGHHLGK
	14257	1011.959	2021.9034	2021.9041	109.26	2.30E–11	YFDSFGDLSSASAIMGNPK
2	**P11517**	Mass, 15972	Score, 2095	Matches 85(85)	Sequences, 13(13)	emPAI, 67.88	
	Hemoglobin subunit beta-2 Rattus norvegicus GN = Hbb2						
	Query	Observed	Mr(expt)	Mr(calc)	Score	Expect	Peptide
	5761	739.4104	738.4031	738.4024	28.51	0.0025	HLDNLK
	8065	912.4783	911.471	911.4712	43.63	0.0001	VHLTDAEK
	8155	459.7562	917.4978	917.4971	41.46	0.00029	ATVSGLWGK
	9911	1090.589	1089.5817	1089.5818	53.78	2.30E–05	VINAFNDGLK
	10208	561.8355	1121.6564	1121.6557	71.86	6.80E–08	VVAGVASALAHK
	10248	563.786	1125.5574	1125.5567	28.79	0.005	LHVDPENFR
	10938	609.8459	1217.6772	1217.6768	72.89	2.20E–07	KVINAFNDGLK
	11335	637.8666	1273.7186	1273.7183	51.57	1.90E–05	LLVVYPWTQR
	12152	699.33	1396.6454	1396.6445	58.4	4.10E–06	EFTPCAQAAFQK
	12274	711.897	1421.7794	1421.7779	63.1	1.60E–06	VVAGVASALAHKYH
	12695	505.5738	1513.6996	1513.6984	27.73	0.0054	GTFAHLSELHCDK
	13339	572.0121	1713.0145	1713.0124	39.19	0.00012	LLGNMIVIVLGHHLGK
	13377	861.4307	1720.8468	1720.8454	93.58	1.80E–09	FGDLSSASAIMGNPQVK
3	**P01946**	Mass, 15319	Score, 1878	Matches, 90(90)	Sequences, 12(12)	emPAI, 43.93	
	Hemoglobin subunit alpha-1/2 Rattus norvegicus GN=Hba1						
	Query	Observed	Mr(expt)	Mr(calc)	Score	Expect	Peptide
	4787	664.287	663.2797	663.2799	32.22	0.0006	NCWGK
	5884	747.3885	746.3812	746.381	33.47	0.0018	VLSADDK
	6652	408.2531	814.4916	814.4912	42.8	0.00015	KVADALAK

Protein							
	6708	818.4412	817.4339	817.4334	24.04	0.028	VDPVNFK
	9269	515.2577	1028.5008	1028.5001	45.21	6.30E–05	MFAAFPTTK
	9852	544.3166	1086.6186	1086.6186	37.59	0.00065	LRVDPVNFK
	10821	602.3326	1202.6506	1202.6507	65.56	1.20E–06	VLSADDKTNIK
	11189	626.8617	1251.7088	1251.7075	89.05	2.80E–09	FLASVSTVLTSK
	12934	786.8738	1571.733	1571.7328	62.23	1.50E–06	IGGHGGEYGEEALQR
	13410	868.4362	1734.8578	1734.8577	68.85	7.30E–07	TYFSHIDVSPGSAQVK
	15156	575.0444	2296.1485	2296.1448	46.15	0.00013	AADHVEDLPGALSTLSDLHAHK
4	**Q00715**	Mass, 13982	Score, 1255	Matches, 51(51)	Sequences, 7(7)	emPAI, 16.05	
	Histone H2B type 1 Rattus norvegicus						
	Query	Observed	Mr(expt)	Mr(calc)	Score	Expect	Peptide
	4797	664.3625	663.3552	663.3551	18.43	0.045	STITSR
	6686	408.733	815.4514	815.4501	34.7	0.0016	EIQTAVR
	6842	414.7141	827.4136	827.4137	42.55	9.70E–05	HAVSEGTK
	8548	477.3055	952.5964	952.5957	38.11	0.00015	LLLPGELAK
	10592	390.2036	1167.589	1167.5884	43.65	0.00016	QVHPDTGISSK
	11281	633.3248	1264.635	1264.6339	29.56	0.0053	KESYSVYVYK
	13451	872.414	1742.8134	1742.812	97.35	5.60E–10	AMGIMNSFVNDIFER
5	**P62804**	Mass, 11360	Score, 1181	Matches, 45(45)	Sequences, 7(7)	emPAI, 9.93	
	Histone H4 Rattus norvegicus GN = Hist1h4b						
	Query	Observed	Mr(expt)	Mr(calc)	Score	Expect	Peptide
	5547	714.3456	713.3383	713.3385	41.44	8.30E–05	TLYGFGG
	8883	495.2927	988.5708	988.5706	45.7	7.70E–05	VFLENVIR
	10315	567.7753	1133.536	1133.5353	37.2	0.00065	DAVTYTEHAK
	10681	590.8146	1179.6146	1179.6135	78.4	5.60E–08	ISGLIYEETR
	11608	655.8549	1309.6952	1309.6952	62.61	1.80E–06	TVTAMDVVYALK
	11721	663.3807	1324.7468	1324.7463	43.17	9.60E–05	DNIQGITKPAIR
	11734	663.8532	1325.6918	1325.6901	62.95	1.60E–06	TVTAMDVVYALK
	12498	489.6064	1465.7974	1465.7963	19.35	0.037	TVTAMDVVYALKR
6	**P15865**	Mass, 21974	Score, 926	Matches, 52(52)	Sequences, 7(7)	emPAI, 2.59	
	Histone H1.4 Rattus norvegicus GN=Hist1h1e						
	Query	Observed	Mr(expt)	Mr(calc)	Score	Expect	Peptide
	6256	392.7374	783.4602	783.4603	37.95	0.00016	KPAAAAGAK
	7669	437.7536	873.4926	873.492	38.94	0.00059	KATGTATPK
	8763	487.3064	972.5982	972.5968	19.54	0.019	SGVSLAALKK
	10082	554.2875	1106.5604	1106.5608	56.04	9.00E–06	ALAAAGYDVEK
	10792	599.838	1197.6614	1197.6605	58.95	4.80E–06	ASGPPVSELITK
	11737	442.9258	1325.7556	1325.7554	32.4	0.0016	KASGPPVSELITK
7	**P0C169**	Mass, 14097	Score, 718	Matches, 23(23)	Sequences, 5(5)	emPAI, 3.55	
	Histone H2A type 1-C Rattus norvegicus						
	Query	Observed	Mr(expt)	Mr(calc)	Score	Expect	Peptide
	1567	425.7671	849.5196	849.5184	23.42	0.0045	HLQLAIR

Protein							
	1733	431.2012	860.3878	860.3875	20.32	0.014	NDEELNK
	3261	472.7701	943.5256	943.524	67.07	1.20E–06	AGLQFPVGR
	18687	966.0891	1930.1636	1930.1615	78.59	1.40E–08	VTIAQGGVLPNIQAVLLPK
	25442	972.5353	2914.5841	2914.5804	74.31	8.20E–08	VGAGAPVYLAAVLEYLTAEILELAGNAAR
8	**P0CC09**	Mass, 14087	Score, 671	Matches, 22(22)	Sequences, 5(5)	emPAI, 3.55	
	Histone H2A type 2-A Rattus norvegicus GN=Hist2h2aa3						
	Query	Observed	Mr(expt)	Mr(calc)	Score	Expect	Peptide
	1567	425.7671	849.5196	849.5184	23.42	0.0045	HLQLAIR
	1733	431.2012	860.3878	860.3875	20.32	0.014	NDEELNK
	3261	472.7701	943.5256	943.524	67.07	1.20E–06	AGLQFPVGR
	18687	966.0891	1930.1636	1930.1615	78.59	1.40E–08	VTIAQGGVLPNIQAVLLPK
	25613	983.8522	2948.5348	2948.5317	86.85	6.90E–09	VGAGAPVYMAAVLEYLTAEILELAGNAAR
9	**P04797**	Mass, 35805	Score, 501	Matches, 10(10)	Sequences, 3(3)	emPAI, 0.3	
	Glyceraldehyde-3-phosphate dehydrogenase Rattus norvegicus GN=Gapdh						
	Query	Observed	Mr(expt)	Mr(calc)	Score	Expect	Peptide
	10287	685.3768	1368.739	1368.7361	72.08	2.00E–07	GAAQNIIPASTGAAK
	11027	778.9102	1555.8058	1555.8029	100.14	3.50E–10	VPTPNVSVVDLTCR
	12207	910.4582	1818.9018	1818.8968	59.72	5.70E–06	IVSNASCTTNCLAPLAK
10	**Q00729**	Mass, 14216	Score, 482	Matches, 39(39)	Sequences, 5(5)	emPAI, 5.92	
	Histone H2B type 1-A Rattus norvegicus GN=Hist1h2ba						
	Query	Observed	Mr(expt)	Mr(calc)	Score	Expect	Peptide
	4797	664.3625	663.3552	663.3551	18.43	0.045	STITSR
	6686	408.733	815.4514	815.4501	34.7	0.0016	EIQTAVR
	6842	414.7141	827.4136	827.4137	42.55	9.70E–05	HAVSEGTK
	8548	477.3055	952.5964	952.5957	38.11	0.00015	LLLPGELAK
	10592	390.2036	1167.589	1167.5884	43.65	0.00016	QVHPDTGISSK
11	**Q06647**	Mass, 23383	Score, 446	Matches, 21(21)	Sequences, 8(8)	emPAI, 2.8	
	ATP synthase subunit O, mitochondrial Rattus norvegicus GN=Atp5o						
	Query	Observed	Mr(expt)	Mr(calc)	Score	Expect	Peptide
	9061	504.7904	1007.5662	1007.5651	22.49	0.0096	TVLNSFLSK
	10374	573.2957	1144.5768	1144.5764	24.79	0.014	YATALYSAASK
	10909	608.8688	1215.723	1215.7227	62.75	9.30E–07	VSLAVLNPYIK
	11586	654.8181	1307.6216	1307.6214	26.26	0.0084	TDPSIMGGMIVR
	12974	528.3076	1581.901	1581.8991	37.98	0.00029	LVRPPVQVYGIEGR
	13903	938.9837	1875.9528	1875.9512	50.08	4.90E–05	FSPLTANLMNLLAENGR
	14291	678.6865	2033.0377	2033.0364	35.54	0.0015	LGNTQGVISAFSTIMSVHR
	15335	1188.604	2375.1934	2375.193	64.91	1.60E–06	GEVPCTVTTAFPLDEAVLSELK
12	**P15999**	Mass, 59717	Score, 358	Matches, 12(12)	Sequences, 5(5)	emPAI, 0.38	
	ATP synthase subunit alpha, mitochondrial Rattus norvegicus GN=Atp5a1						
	Query	Observed	Mr(expt)	Mr(calc)	Score	Expect	Peptide
	5733	423.2588	844.503	844.5018	38.23	0.00071	STVAQLVK
	6124	439.217	876.4194	876.4189	31.77	0.0027	ISEQSDAK

Protein							
	8969	586.3209	1170.6272	1170.6245	51.74	2.50E–05	VVDALGNAIDGK
	10146	668.8441	1335.6736	1335.6711	44.06	0.00019	EIVTNFLAGFEP
	11081	788.3985	1574.7824	1574.7788	75.59	1.10E–07	ILGADTSVDLEETGR
13	**Q6LED0**	Mass, 15394	Score, 338	Matches, 23(23)	Sequences, 4(4)	emPAI, 2.3	
	Histone H3.1 Rattus norvegicus						
	Query	Observed	Mr(expt)	Mr(calc)	Score	Expect	Peptide
	5576	715.4102	714.4029	714.4024	34.16	0.0016	DIQLAR
	6889	416.2504	830.4862	830.4861	50.19	4.10E–05	STELLIR
	7256	850.431	849.4237	849.4232	49.8	3.90E–05	EIAQDFK
	9295	516.8012	1031.5878	1031.5876	21.29	0.023	YRPGTVALR
14	**P63039**	Mass, 60917	Score, 288	Matches, 7(7)	Sequences, 4(4)	emPAI, 0.3	
	60 kDa heat shock protein, mitochondrial Rattus norvegicus GN=Hspd1						
	Query	Observed	Mr(expt)	Mr(calc)	Score	Expect	Peptide
	8933	617.3018	1232.589	1232.5885	51.45	2.80E–05	VGGTSDVEVNEK
	20403	715.7147	2144.1223	2144.1221	56.51	8.50E–06	ALMLQGVDLLADAVAVTMGPK
	22880	818.796	2453.3662	2453.3629	60.62	1.40E–06	TALLDAAGVASLLTTAEAVVTEIPK
	25108	947.5204	2839.5394	2839.543	62.63	9.30E–07	TALLDAAGVASLLTTAEAVVTEIPKEEK
15	**P0C0S7**	Mass, 13545	Score, 272	Matches, 13(13)	Sequences, 3(3)	emPAI, 0.96	
	Histone H2A.Z Rattus norvegicus GN=H2afz						
	Query	Observed	Mr(expt)	Mr(calc)	Score	Expect	Peptide
	7274	425.767	849.5194	849.5184	29.45	0.0011	HLQLAIR
	8476	472.7698	943.525	943.524	59.27	7.80E–06	AGLQFPVGR
	10178	559.7829	1117.5512	1117.5503	41.73	0.00033	GDEELDSLIK
16	**Q09073**	Mass, 32880	Score, 164	Matches, 6(6)	Sequences, 3(3)	emPAI, 0.33	
	ADP/ATP translocase 2 Rattus norvegicus GN=Slc25a5						
	Query	Observed	Mr(expt)	Mr(calc)	Score	Expect	Peptide
	7335	428.7483	855.482	855.4814	35.07	0.0005	TAVAPIER
	10954	610.3386	1218.6626	1218.6608	43.09	0.00017	DFLAGGVAAAISK
	12409	723.8749	1445.7352	1445.7343	63.47	2.20E–06	YFPTQALNFAFK
17	**P04636**	Mass, 35661	Score, 161	Matches, 3(3)	Sequences, 2(2)	emPAI, 0.19	
	Malate dehydrogenase, mitochondrial Rattus norvegicus GN=Mdh2						
	Query	Observed	Mr(expt)	Mr(calc)	Score	Expect	Peptide
	5833	537.2957	1072.5768	1072.5764	28.28	0.007	IQEAGTEVVK
	16994	897.0486	1792.0826	1792.0822	93.25	4.70E–10	VAVLGASGGIGQPLSLLLK
18	**P10719**	Mass, 56318	Score, 119	Matches, 3(3)	Sequences, 3(3)	emPAI, 0.12	
	ATP synthase subunit beta, mitochondrial Rattus norvegicus GN = Atp5b						
	Query	Observed	Mr(expt)	Mr(calc)	Score	Expect	Peptide
	12349	718.3795	1434.7444	1434.7467	55.6	1.50E–05	FTQAGSEVSALLGR
	14162	994.5206	1987.0266	1987.0262	59.15	5.00E–06	AIAELGIYPAVDPLDSTSR
	8952	499.2514	996.4882	996.4876	35.02	0.00077	LSYNTASNK
19	**Q3KR86**	Mass, 67135	Score, 82	Matches, 3(3)	Sequences, 3(3)	emPAI, 0.15	
	Mitochondrial inner membrane protein (Fragment) Rattus norvegicus GN=Immt						

Protein							
	Query	Observed	Mr(expt)	Mr(calc)	Score	Expect	Peptide
	702	404.714	807.4134	807.4127	27.88	0.0064	AFDSAVAK
	5879	538.2546	1074.4946	1074.4941	33.7	0.00083	SEIQAEQDR
	8883	616.2936	1230.5726	1230.5728	52.8	1.20E–05	YSTSSSSGVTAGK
20	**P19527**	Mass, 61298	Score, 74	Matches, 6(6)	Sequences, 4(4)	emPAI, 0.23	
	Neurofilament light polypeptide Rattus norvegicus GN=Nefl						
	Query	Observed	Mr(expt)	Mr(calc)	Score	Expect	Peptide
	1996	437.2246	872.4346	872.4352	28.26	0.0043	GADEAALAR
	4401	501.759	1001.5034	1001.5029	34.67	0.0012	QLQELEDK
	5557	531.2589	1060.5032	1060.5036	30.6	0.0033	LAAEDATNEK
	6814	561.2956	1120.5766	1120.5764	22.84	0.025	EYQDLLNVK
21	**P16036**	Mass: 39419	Score:70	Matches: 2(2)	Sequences: 1(1)	emPAI, 0.08	
	Phosphate carrier protein, mitochondrial Rattus norvegicus GN = Slc25a3						
	Query	Observed	Mr(expt)	Mr(calc)	Score	Expect	Peptide
	5301	523.7833	1045.552	1045.5516	42.38	0.00031	GSTASQVLQR
	5302	523.7834	1045.5522	1045.5516	47.53	9.20E–05	GSTASQVLQR
22	**P48721**	Mass, 73812	Score, 59	Matches, 2(2)	Sequences, 2(2)	emPAI, 0.09	
	Stress-70 protein, mitochondrial Rattus norvegicus GN = Hspa9						
	Query	Observed	Mr(expt)	Mr(calc)	Score	Expect	Peptide
	4786	510.7329	1019.4512	1019.452	31.29	0.0014	DSETGENIR
	8885	616.3359	1230.6572	1230.6568	45.12	0.00015	QAASSLQQASLK
23	**D3ZAF6**	Mass, 10446	Score, 58	Matches, 2(2)	Sequences, 1(1)	emPAI, 0.33	
	ATP synthase subunit f, mitochondrial Rattus norvegicus GN=Atp5j2						
	Query	Observed	Mr(expt)	Mr(calc)	Score	Expect	Peptide
	11091	619.8123	1237.61	1237.6091	35.17	0.0011	DFTPSGIAGAFR
24	**P12839**	Mass, 95734	Score, 50	Matches, 5(5)	Sequences, 3(3)	emPAI, 0.11	
	Neurofilament medium polypeptide Rattus norvegicus GN=Nefm						
	Query	Observed	Mr(expt)	Mr(calc)	Score	Expect	Peptide
	1541	424.7401	847.4656	847.4651	34.19	0.0021	TDISTALK
	6814	561.2956	1120.5766	1120.5764	22.84	0.025	EYQDLLNVK
	11986	469.209	1404.6052	1404.6045	20.82	0.014	VEEHEETFEEK
25	**Q5XI78**	Mass, 116221	Score, 50	Matches, 2(2)	Sequences, 1(1) emPAI, 0.03		
	2-oxoglutarate dehydrogenase, mitochondrial Rattus norvegicus GN=Ogdh						
	Query	Observed	Mr(expt)	Mr(calc)	Score	Expect	Peptide
	15230	830.4722	1658.9298	1658.9283	39.81	0.00024	IEQLSPFPFDLLLK
26	**Q9ER34**	Mass, 85380	Score, 50	Matches, 3(3)	Sequences, 2(2)	emPAI, 0.08	
	Aconitate hydratase, mitochondrial Rattus norvegicus GN=Aco2						
	Query	Observed	Mr(expt)	Mr(calc)	Score	Expect	Peptide
	4084	494.7566	987.4986	987.4985	33.57	0.0018	VDVSPTSQR
	5713	534.2777	1066.5408	1066.5407	22.74	0.014	NTIVTSYNR
27	**D3ZBN0**	Mass, 22635	Score, 43	Matches, 3(3)	Sequences, 2(2)	emPAI, 0.32	
	Histone H1.5 Rattus norvegicus GN=Hist1h1b						

Protein							
	Query	Observed	Mr(expt)	Mr(calc)	Score	Expect	Peptide
	8274	547.2804	1092.5462	1092.5451	28.01	0.0055	ALAAGGYDVEK
	9390	606.8467	1211.6788	1211.6761	24.64	0.0077	ATGPPVSELITK
28	**P17764**	Mass, 44666	Score, 42	Matches, 2(2)	Sequences, 1(1)	emPAI, 0.07	
	Acetyl-CoA acetyltransferase, mitochondrial Rattus norvegicus GN=Acat1						
	Query	Observed	Mr(expt)	Mr(calc)	Score	Expect	Peptide
	13965	815.1015	2442.2827	2442.2835	30.5	0.0028	IAAFADAAVDPIDFPLAPAYAVPK
29	**Q63617**	Mass, 111220	Score, 42	Matches, 3(3)	Sequences, 2(2)	emPAI, 0.06	
	Hypoxia up-regulated protein 1 Rattus norvegicus GN=Hyou1						
	Query	Observed	Mr(expt)	Mr(calc)	Score	Expect	Peptide
	5477	529.2618	1056.509	1056.5087	25	0.0062	EVEEEPGLR
	13694	768.4272	1534.8398	1534.8395	27.72	0.0053	DAVIYPILVEFTR
30	**Q05962**	Mass, 32968	Score, 33	Matches, 2(2)	Sequences, 1(1)	emPAI, 0.1	
	ADP/ATP translocase 1 Rattus norvegicus GN=Slc25a4						
	Query	Observed	Mr(expt)	Mr(calc)	Score	Expect	Peptide
	1634	428.7482	855.4818	855.4814	26.28	0.0038	TAVAPIER